International Journal of Concrete Structures and Materials
Vol.9, No.4, pp.463–473, December 2015
DOI 10.1007/s40069-015-0115-6
ISSN 1976-0485 / eISSN 2234-1315

Evaluation of Internally Cured Concrete Pavement Using Environmental Responses and Critical Stress Analysis

Kukjoo Kim*, and Sanghyun Chun

(Received May 26, 2015, Accepted September 25, 2015, Published online October 20, 2015)

Abstract: Three full-scale instrumented test slabs were constructed and tested using a heavy vehicle simulator (HVS) to evaluate the structural behavior of internally cured concrete (ICC) for use in pavements under Florida condition. Three mix designs selected from a previous laboratory testing program include the standard mixture with 0.40 water-cement ratio, the ICC with 0.32 water-cement ratio, and the ICC mixture with 0.40 water-cement ratio. Concrete samples were prepared and laboratory tests were performed to measure strength, elastic modulus, coefficient of thermal expansion and shrinkage properties. The environmental responses were measured using strain gages, thermocouples, and linear variable differential transformers instrumented in full-scale concrete slabs. A 3-D finite element model was developed and calibrated using strain data measured from the full-scale tests using the HVS. The results indicate that the ICC slabs were less susceptible to the change of environmental conditions and appear to have better potential performance based on the critical stress analysis.

Keywords: internally cured concrete slab, rigid pavements, full-scale HVS testing, stress analysis, pavement instrumentation, finite element analysis.

1. Introduction

1.1 Background

In recent years, the high-strength-high-performance concrete (HSHPC) has been widely used for a rapid repair of concrete bridge decks and concrete pavements. This type of concrete usually shows very high early chemical shrinkage that likely result in shrinkage cracking. Also, the HSHPC generates more heat and therefore naturally prone to create more premature cracking. These early cracks are one of the primary causes for promoting the concrete structural deficiencies or even failures.

The internally cured concrete (ICC) is one potential way to mitigate the problems with the HSHPC by supplying an internal water source for concrete. Two internal reservoirs of water have been recently developed. One is based on the use of light-weight aggregate (LWA), while the other is the use of superabsorbent polymers (SAP). Since the internal curing agents are a highly porous material, an each particle of internal curing agent acts like a small reservoir inside the concrete when it is saturated. This will provide water to the surrounding cement paste during the hydrating period. The water to be released to the paste by incorporating internal curing agents into a normal concrete helps more degree of hydration and reduces a self-desiccation (Weber and Reinhardt 1997; Cusson and Hoogeveen 2008). Consequently, the ICC is able to lessen the cracking tendency of the concrete at the early age. In addition, the internal curing results in other benefits including increased cement hydration, higher strength, reduced permeability, and higher durability (Bentz et al. 2005).

More recently, the ICC has been successfully used for a pavement project in Hutchins, Texas (Villarreal and Crocker 2007). They found that internal curing pavement achieved 7-day flexural strength up to 90–100 % of the required 28-day flexural strength due to an improved hydration process. However, previous research regarding the performance of concrete pavement in Florida indicated that the optimal concrete mixture for concrete pavement was not necessarily a concrete with a high flexural strength, but a concrete with a proper combination of low modulus of elasticity, low coefficient of thermal expansion, and adequate flexural strength (Tia et al. 1991). Also, it was reported that the percentage of cracked slabs increased with an increase in modulus of elasticity of the concrete based on the field study for I-75 concrete pavements in Sarasota and Manatee Counties in Florida (Tia et al. 1989).

Although the benefits of the ICC for use in pavement have been evidenced in the literatures and some field experiences, the structural behavior and performance characteristics of the ICC slabs for Florida condition including typical temperature differentials and maximum loading condition have not been thoroughly evaluated. Therefore, there is a still need to assess the effect of the ICC on change in structural and

Engineering School of Sustainable Infrastructure and Environment, University of Florida, Gainesville, FL 32611, USA.
*Corresponding Author; E-mail: klauskim@ufl.edu

environmental critical responses that plays a significant role on the ICC pavement performance in the field. This paper will demonstrate the evaluation of the ICC and standard mix pavements based on the results of the response measurements using full-scale field tests, the development of finite element (FE) model, and the comparison between predicted and measured responses.

1.2 Objectives and Scope

The primary objective of this study is to evaluate the performance and applicability of the ICC using lightweight aggregates (LWAs) for use in pavements under Florida conditions using a laboratory and a full-scale field testing program. The instrumented concrete slabs were constructed and tested using a heavy vehicle simulator (HVS). Also, a three-dimensional FE analysis was conducted to assess the potential performance of the ICC.

2. Effect of Internal Curing on Mechanical Behavior of Concrete

In general, the internal curing will produce better results in terms of strength and elastic modulus due to an increase in the degree of hydration for the cement paste. The interfacial bonds between cement gel and aggregates are strengthened by the increased hydration activities. This usually helps improve strength characteristics of the concrete including compressive, tensile or flexural strength. However, increasing the amount of LWA can potentially lead to a reduction of compressive strength when the same water-cement ratio is used (de Sensale and Goncalves 2014; Lotfy et al. 2015). Therefore, it is imperative to control the LWA's amount, size, and porosity for ICC mixtures.

The internal curing could provide a decreased early strength of concrete and also an increased ultimate strength. If the supplementary cementitious materials are used, this ultimate strength will exhibit even better performance (Bentz and Weiss 2011). In addition, elastic modulus is an important property of concrete usually overlooked by the concrete designers. It is generally agreed that performance of concrete is influenced by the concrete strength. However, the analysis of the concrete strength only is not able to fully describe the quality and performance of concrete. Weiss et al. indicated that a decreased modulus of elasticity is capable of reducing the cracking potential of the concrete. The concrete with a lower modulus of elasticity can be considered as more flexible than the one with greater modulus. Therefore, less rigidity of the mixture can provide a better performance and reduced early age cracking caused by thermal displacement, autogenous shrinkage, drying shrinkage, and restrained shrinkage (Weiss et al. 1999).

The elastic modulus of concrete is affected by the elastic moduli of its constituents. The LWAs usually have lower elastic modulus than the typical aggregates and consequently, the LWA concrete has a lower elastic modulus as compared to a mixture with conventional aggregates. The elastic modulus of concrete containing LWA at an early-age shows lower values than normal concrete, and the influence of LWA is weaker than that of compressive strength. The lower values of elastic modulus are related to a reduction in cracking potential because the residual stresses are decreased (Bentz and Weiss 2011). Byard and Schindler characterized the modulus of elasticity for different mixtures and established that the reduced stiffness of LWA can lower the modulus of elasticity of the concrete when LWAs were incorporated into the concrete (Byard and Schindler 2010).

Curling and warping occur as a result of differences in temperature and moisture gradients throughout the thickness of a concrete slab and can cause slabs to either curl up or curl down. The distortions resulting from temperature gradients are called curling, and the distortions due to moisture gradient are called warping. Concrete slab with higher temperature and moisture gradient will lead a higher potential damage by the effects of curling and warping. A reduction of warping and curling can be achieved by maintaining higher and more uniform relative humidity across the concrete slab (Mehta and Monteiro 2013). Also, the LWA is able to reduce curling and warping of concrete as the water drawn from the LWA pores provides better hydration and high relative humidity (Schlitter et al. 2010). Previous studies indicate that approximately 70 % reduction in warping can be perceived when the concrete has a high percentage of relative humidity (Wei and Hansen 2008).

3. Pavement Response Measurements for ICC Slab Using Full-Scale Field Test

The full-scale ICC test slabs were constructed over an existing two-inch thick asphalt surface of an accelerated pavement testing (APT) facility housed at the FDOT State Materials Research Park. The asphalt layer was placed over a 26.67 cm (10.5 in.) limerock base which acted as a leveling course and provided firm and consistent foundation for the concrete slabs. This test track consisted of three 3.7 m by 4.9 m (12 ft by 16 ft) and 23 cm (9 in.) in thickness test slabs with no dowel bar application. A vibrating leveling bar was used to level off the concrete surface of the test slab. A broom was passed over the concrete surface to produce a rough surface texture before it hardened and then a curing compound was applied over the top and sides of the slabs with manufacturer's recommended application rate. The ICC-1 slab was constructed on December 9, 2014 and tested after 87 days. The standard and the ICC-2 slabs were both constructed on December 17, 2014 and HVS loading was applied after 86 and 82 days, respectively.

3.1 Instrumentation Layout and Installation

Figure 1 shows the instrumentation layout for test sections. The locations for the dynamic gages were selected based on the anticipated critical responses of the test slab. At the each gage location, two embedded strain gages were placed at a depth of 2.54 cm (1 in.) from the concrete surface, and 2.54 cm (1 in.) from the bottom of the concrete layer. This can be achieved by securing the gages between two nylon rods to

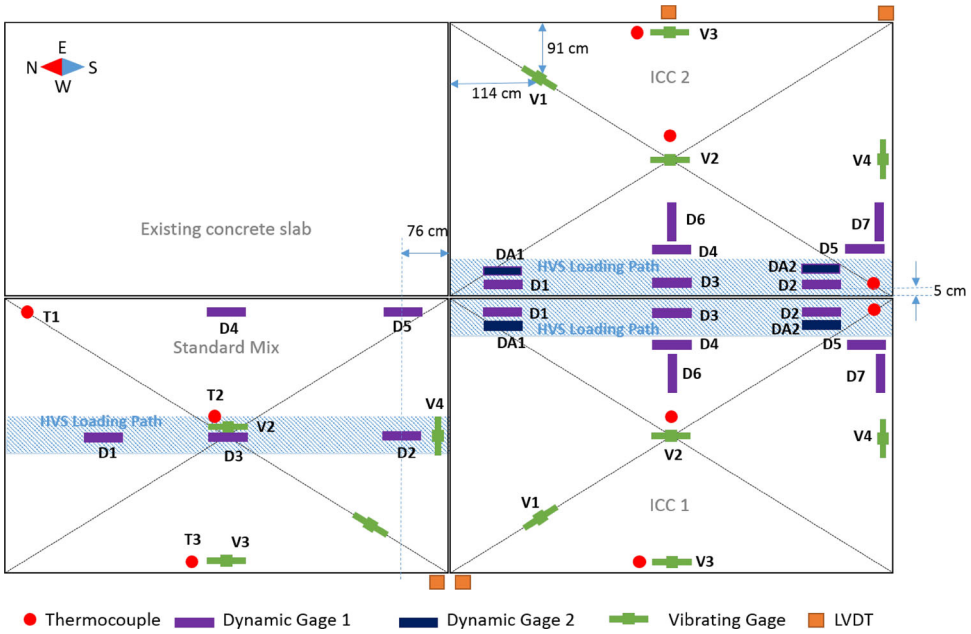

Fig. 1 Instrumentation layout.

reduce the thermal effect on gage readings. Six strain gages were installed on the wheel path in the longitudinal direction. Two of them were placed at mid-edge of the slab, and others were located at 76.2 cm (30 in.) from each joint. For ICC slabs, four additional different types of strain gages were place on the wheel path for more accurate strain readings and comparison of each reading as shown in Fig. 1. To protect the gages during concrete placement, 30.5 cm (12 in.) diameter PVC buckets without bottom plate were used around the strain gages. The concrete was then placed manually around the strain gages inside the PVC buckets and the PVC buckets pulled out vertically to remove them.

Thermocouple wire set consisted of eight wire, which were fixed on a PVC rod and placed at depths of 2.54, 5.08, 7.62, 11.43, 15.24, 17.78, and 20.32 cm (1, 2, 3, 4.5 6, 7, and 8 in.) from the surface of concrete slab. At each of the location, a thermocouple was also installed in the asphalt layer at a depth of 2.54 cm (1 in.) from the top of the asphalt layer, or at a depth of 25.4 cm (10 in.) from the concrete surface. Three sets of thermocouple wires were placed to monitor the temperature distribution for each test slab. One set of thermocouple was installed at the slab corner on the HVS wheel path. Other two sets of thermocouples were installed at the slab center and at the mid-edge of slab, respectively.

3.2 Concrete Mixture Design

The mix designs of concrete used for the three test slabs are presented in Table 1. The standard mix design is the one typically used for concrete pavements in Florida. It received a target cement content of 326.1 kg/m^3 (549.6 lb/yd^3) of concrete, and a water-cement ratio of 0.40. The ICC-1 test slab used a concrete mix design that includes the cement content increased to 408.2 kg/m^3 (688.0 lb/yd^3), while the water-cement ratio reduced to 0.32. Lastly, the ICC-2 test slab used a concrete mix design that received the same cement content and water-cement ratio with the standard mix design, while the fine aggregates are replaced by LWA.

The concretes used in the APT test slabs were produced by Argos concrete plant in Gainesville, Florida. The LWA was prepared in accordance with procedure documented in ASTM C1761. The LWA pile was sprinkled with water for one week before batching to ensure the saturated condition. Standard procedures for adjusting excess water were conducted similarly to typical coarse aggregate. They were mixed in a central mix plant and transported to the test site by a concrete delivery truck. The transit time from the mixing plant to the job site was less than 30 min.

The types and sources of the cement, fly ash, coarse aggregate, conventional fine aggregate, lightweight aggregate, and admixture used are shown in Table 2. Local tap water was used for mixing water.

3.3 Concrete Mixture Properties

The concrete samples were obtained from the concrete truck before the placement of concrete in order to perform slump, unit weight, temperature, and air content tests. Fresh concrete properties are shown in Table 3.

The compressive strength, elastic modulus, flexural strength and drying shrinkage (ASTM C39, C469, C78, and C157) data for the hardened concrete samples at 28 days are presented in Table 4. It is noted that even though the standard mix and the ICC-2 mix received the same cement content in the mix design, the ICC-2 mix showed a slightly lower compressive strength than the standard mix due to the effect of the LWA. Also, the ICC-1 mix exhibited a higher compressive strength likely due to the effects of higher cement content and lower water-cement ratio. The average drying shrinkage from six 76 mm × 76 mm × 286 mm prisms for the three concrete mixtures are also shown in Table 4. It can be seen that the ICC mixtures have lower drying shrinkage than the standard mixture.

Table 1 Mix designs of concrete used in test slabs.

Material	Mix designs		
	Standard mix	ICC-1	ICC-2
Cement (kg/m^3)	326.1	408.2	326.1
Fly ash (kg/m^3)	81.5	102.0	81.5
Coarse aggregate (kg/m^3)	971.7	1013.6	971.7
Sand (kg/m^3)	696.9	238.9	444.9
Light-weight aggregate (kg/m^3)	–	184.6	147.4
Air entrainer (kg/m^3)	0.0	0.4	0.0
Water reducer admixture (kg/m^3)	1.0	1.6	1.0
High-rage water reducer admixture (kg/m^3)	0.3	1.3	0.2
Water (kg/m^3)	163.0	163.2	163.0
water-cement ratio	0.4	0.32	0.4

Table 2 Mix proportions types and sources of test slabs.

Material	Specific gravity	Absorption (%)	Fineness modulus	Sources
Cement	3.15	–	–	Florida Rock Company
Coarse aggregate	2.43[a]	5.0	–	Brooksville, FL
Sand	2.63[a]	0.5	2.63	Branford, FL
Light-weight aggregate	1.54[a]	25.2	4.29	Big River Industries Inc., LA
Fly ash	2.40	–	–	Florida Rock Company

[a] Saturated surface-dry specific gravity

Table 3 Fresh concrete properties.

Test property	Mix type		
	Standard mix	ICC-1	ICC-2
Slump (mm)	146	89	159
Unit weight (kg/m^3)	2281	2137	2175
Temperature (°C)	22	26	23
Air (%)	1.0	3.1	1.7

Table 4 Compressive strength, elastic modulus, flexural strength, and drying shrinkage data.

Test	Mix type		
	Standard mix	ICC-1	ICC-2
Compressive strength (MPa)	47.1	54.1	45.6
Modulus of elasticity (MPa)	30,682	26,890	26,200
Modulus of rupture (kPa)	4999	5640	4861
Drying Shrinkage (ε)			
At 28 days	3.7×10^{-4}	3.1×10^{-4}	3.8×10^{-4}
At 91 days	5.3×10^{-4}	3.8×10^{-4}	5.0×10^{-4}

3.4 HVS Loading and Data Acquisition

Since the most critical loading condition is that the wheel load is applied along the edge of the concrete slab. Thereby, this loading condition was used for application of the HVS loading to the ICC-1 and ICC-2 test slabs as shown in Fig. 1. For the standard mix slab, due to the constraint imposed by the adjacent slab, the HVS loading had to be applied along the center line of the slab. During the HVS load application, dynamic strain data from the tested slab were recorded with every 15 min interval, for 30 s each time, and at a sampling rate of 800 Hz for each strain gage. Also, the temperature data were collected with five minutes intervals.

4. Analysis of Measured Pavement Responses

Because of the extreme sensitivity of critical stresses in concrete pavements to environmental loadings, it is imperative to understand the behavior of concrete slabs under environmental loadings including temperature gradients, curling movement, and environmental strains. To allow measurements of environmental responses, the embedded sensors including thermocouples and strain gages were used. These data, environmental responses before HVS loading applied, were collected and analyzed herein.

4.1 Temperature Measurements

The temperature gradients in the test slab were monitored using instrumented thermocouples at different depths. Figure 2 illustrates a typical hourly slab temperature distribution curve. Data was collected during Jan. 12 to Feb. 2 of 2015. As shown in Fig. 2, temperature distribution along the thickness of the slab is nonlinear at certain times of the day. The maximum positive temperature differential for the ICC slab was about 7.8 °C (14 °F) at 3–4 PM, while the maximum negative temperature differential was −6.7 °C (−12 °F) at 11–12 PM. However, for the standard mix slab, the maximum temperature gradients were 5.0 °C (+9 °F) and −4.4 °C (−8 °F) at the same time.

This indicates that the temperature differentials of the ICC slab are higher than that of the standard mix slab. It can be explained that the addition of LWA as an internal curing agent increase the degree of hydration which results in a more dense microstructure and the more dense microstructure results in a decrease in the thermal conductivity of the concrete (Schlitter et al. 2010). This low thermal conductivity of the ICC slab prevents the ICC slab from the fast temperature change inside the concrete slab that may lead to the higher temperature differentials in ICC slabs. In addition, the hourly temperature variation at the middle of AC layer under the standard mix slab is higher than that under the ICC slab as shown in Fig. 2. The low thermal conductivity of ICC slab may also influence the smaller temperature variation in AC layer under the ICC slab compared to that under the standard mix slab.

4.2 Curling Measurements

Curling was measured directly using LVDTs at the corner of the slabs. The LVDTs were installed on the slab using Invar Bar which has very low coefficient of thermal expansion to minimize the temperature effect on vertical movement readings. In this study, only the changes in the elevation at the LVDT locations were measured since the vertical measurements stated after the slabs hardened. Therefore, the curling deflection shown in Fig. 3 do not indicate the actual curling even though it is relative to the first measurement. It should be noted that the actual curling of the slabs may be higher or lower depending upon the time of first measurement. The higher magnitude of curling was observed for the standard mix slab compared to the ICC slabs. Based on this result, it can be concluded that the curling stress in the standard mix slab is higher than the ICC slab, if slab dimension, self-weight, and temperature differentials are the same.

4.3 Strain Measurements

Strain measurement was accomplished using Vibrating Wire Gages manufactured by Geokon Model 4200. The most significant issue of the environmental strain analysis involved the offsets of the strain gages. To solve this problem, only the relative strain changes at 10 °C (50 °F) were measured. As shown in Fig. 4, the standard mix slab exhibits relatively higher environmental strain changes that may cause the higher environmental stresses since the standard mix slab usually shows higher elastic modulus than the ICC slabs.

5. Finite Element Analysis

5.1 Meshing and Material Properties

A three-dimensional FE model was developed to predict the maximum stress on the test slabs that enables to evaluate the potential performance of the ICC and the standard mix. The ADINA (version 9.0) finite element program was used to analyze the anticipated maximum stresses on the test slabs. The ADINA program has been widely used in previous research to evaluate the critical responses of the concrete slab. In this study, two types of elements were used to develop the mesh including the hexahedrons elements and the translational spring elements. The hexahedrons elements are defined by eight nodes with three degrees of freedom (i.e. translations in the x-, y-, and z-directions). The spring elements were used to model the load transfer across the joints between two adjoining concrete slab. The spring elements also have three degrees of freedom. The size of the meshes, number of elements, and suitable dimension were determined in consideration with optimized computation times and engineering efforts. Figure 5 presents a 3-D FE model developed for the analysis of the test slabs.

The subgrade materials are modeled as isotropic and linearly elastic material characterized by their elastic modulus and Poisson's ratio. The material properties used in FE

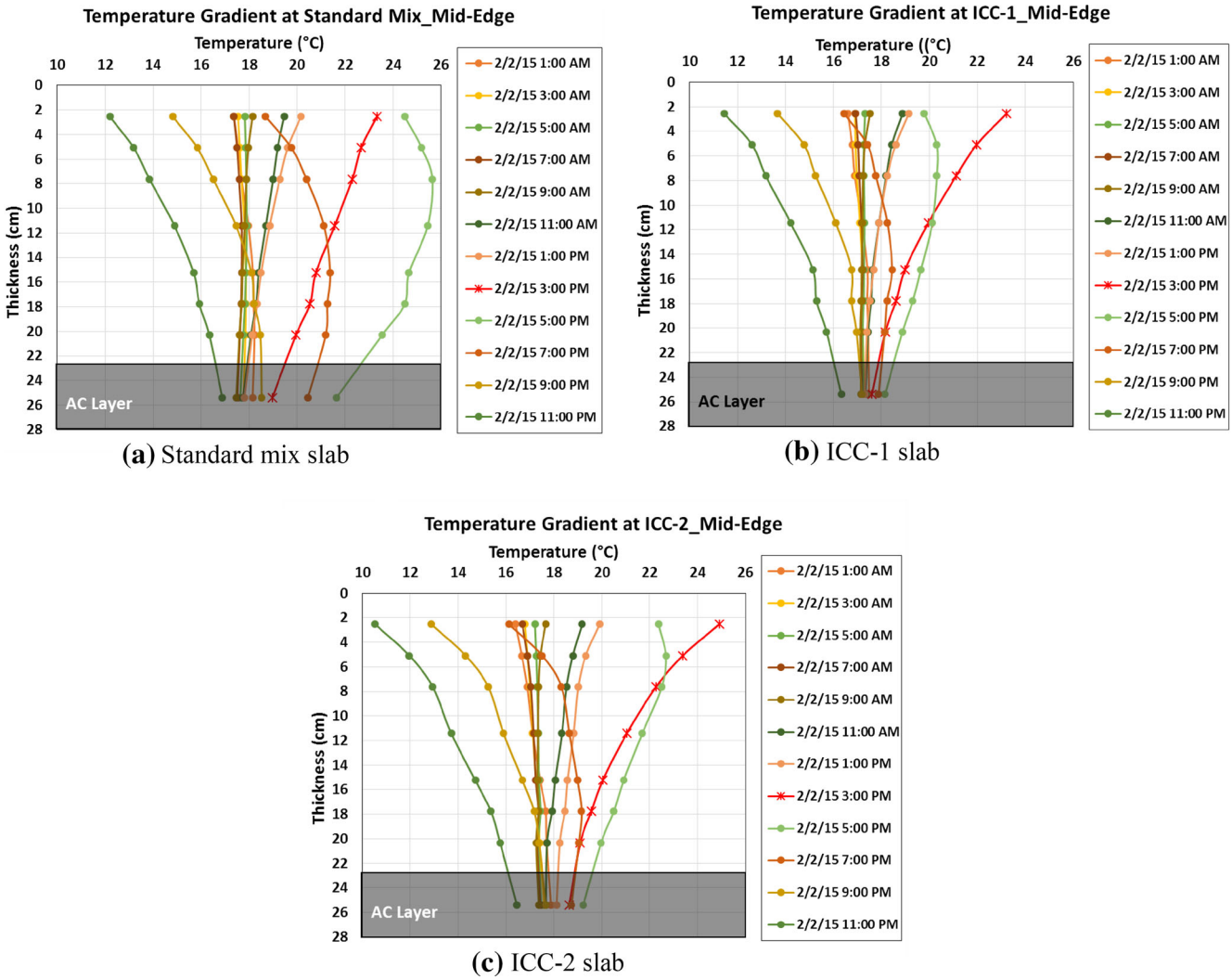

Fig. 2 Temperature distribution across the slab thickness at the mid-edge of the slab.

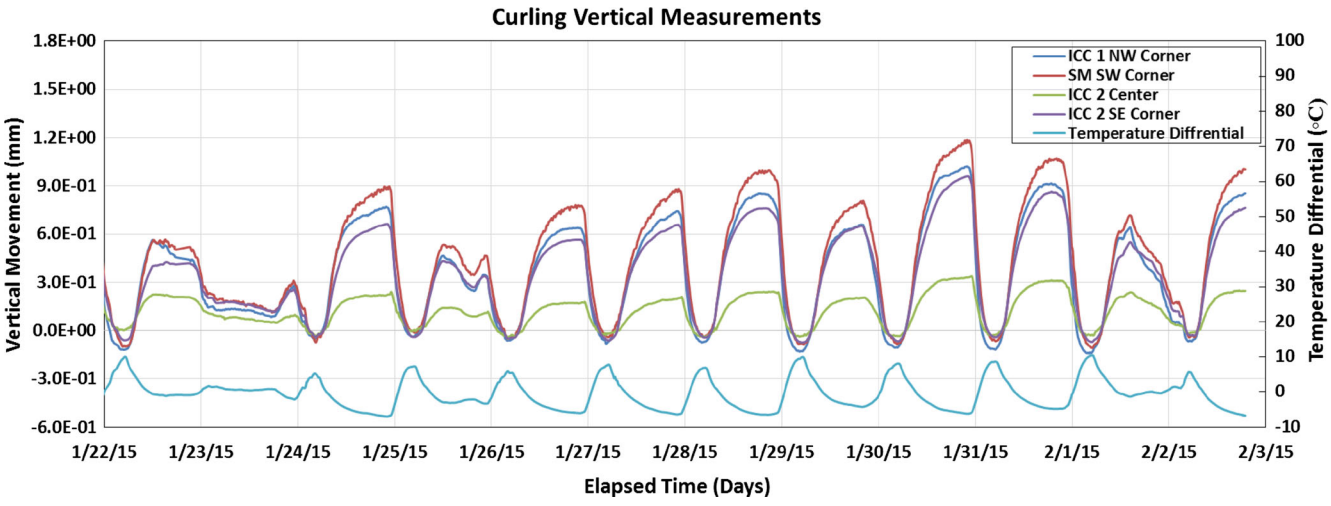

Fig. 3 Measured vertical movements.

analysis were estimated by back-calculation using the FWD data. The elastic modulus, coefficient of thermal expansion and Poisson's ratio of the concrete were initially estimated from the results of laboratory tests on the sampled concrete. The elastic modulus of subgrade and the spring stiffnesses of joint and edges were estimated by back-calculation of the FWD deflection data used as ADINA inputs for FE model developed. Pavement surface deflection basins induced by a

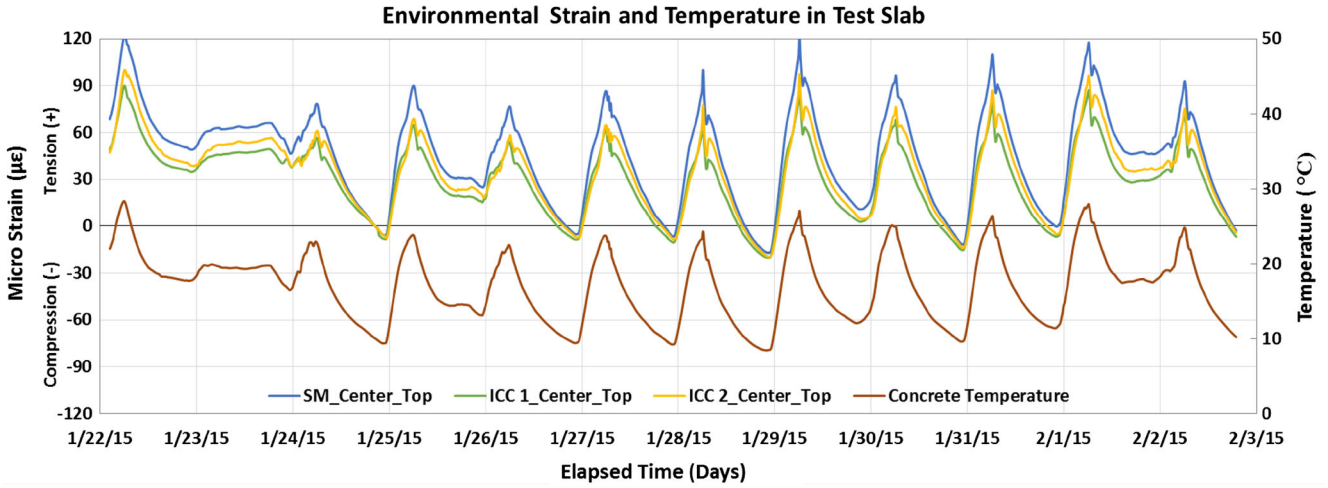

Fig. 4 Measured environmental strain.

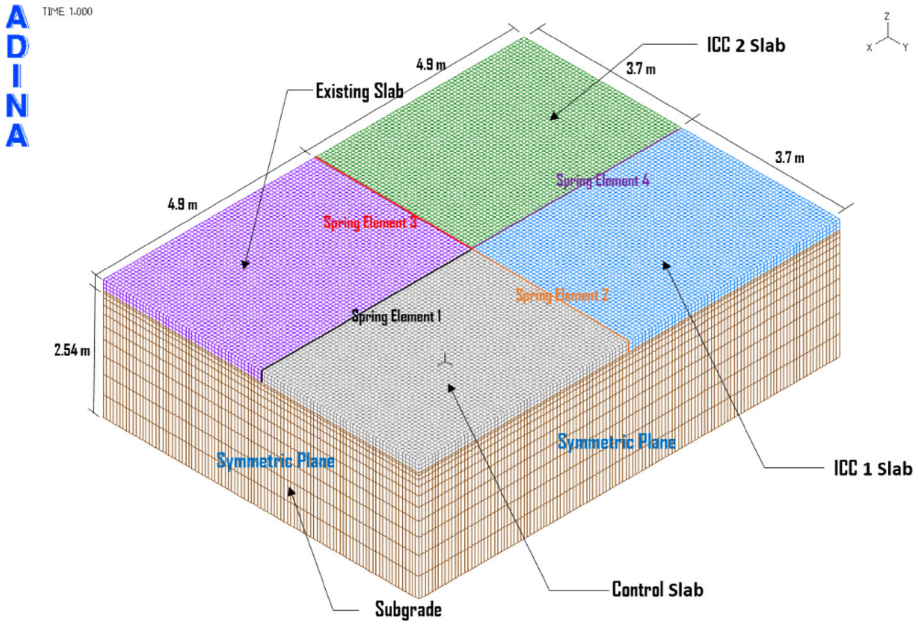

Fig. 5 3-D finite element model for test slabs.

40 kN (9-kip) FWD applied load were used to estimate the values of the elastic modulus for the subgrade and the stiffness of the springs used to model the load transfer at the joints. Table 5 presents a summary of model parameters estimated from laboratory and back-calculation in this study.

5.2 Boundary Condition and Slab Joints

The double symmetry of the geometry about x- and y-axes with large enough dimensions at a depth of 254 cm (100 in.) was selected to simulate the real boundary condition. The bottom of the subgrade layer was modeled as fixed with z- direction. Load transfer across the joint between two adjacent slabs is modeled by translational spring element connected to the nodes of the finite elements along the joint. Three values of spring constants were used to represent the stiffnesses along x-, y-, and z-direction.

5.3 Loading Configuration and Temperature Effects

The critical loading condition considered in this analysis to determine the maximum stresses in the test slab if it were loaded by a 98 kN (22-kip) axle load which is the maximum legal single axle load in Florida applied at two critical loading positions, including (1) at the middle of the slab edge and (2) at the slab corner, are shown in Fig. 6. Three different temperature differentials of concrete layer were also considered including (1) temperature differential of −5.6 °C (−10 °F), which represents a typical severe condition at night, (2) temperature differential of 11.1 °C (+20 °F), which represents a typical severe condition in the daytime, (3) no temperature differential. To evaluate the most extreme condition, no load transfer effects were considered for analysis.

Table 5 Material properties in FEM model.

Parameters used in ADINA	Standard mix	ICC-1	ICC-2
Elastic modulus of concrete (MPa)	30,628	26,890	26,200
Density of concrete (kg/m^3)	2215	2081	2089
Coefficient of thermal expansion (m/m/°C)	7.965×10^{-6}	7.630×10^{-6}	7.630×10^{-6}
Poisson's ratio	0.2	0.2	0.2
Elastic modulus of subgrade (MPa)	724	724	724
Spring constant for load transfer (kN/m)			
Trans. joint X	1.75×10^3	1.75×10^3	–
Trans. joint Y	1.75×10^3	1.75×10^3	–
Trans. joint Z	1.75×10^4	1.75×10^5	–
Long. joint X	1.75×10^3	–	1.75×10^3
Long. joint Y	1.75×10^3	–	1.75×10^3
Long. joint Z	1.75×10^5	–	1.75×10^4

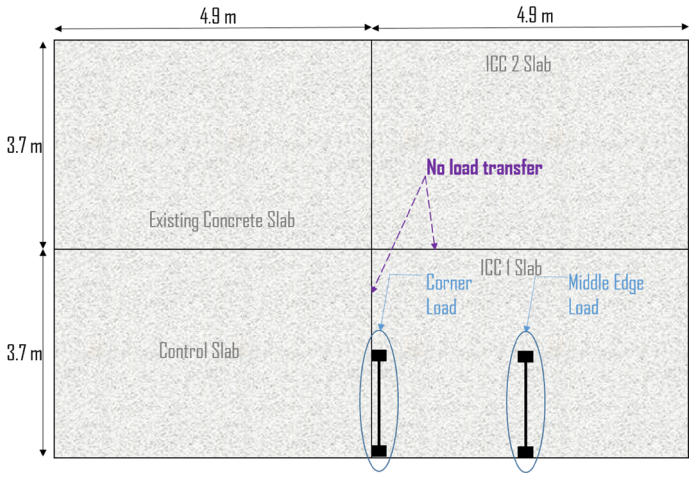

Fig. 6 Critical loading conditions.

5.4 FE Model Validation

In order to verify the parameters used for ADINA model, the measured strains from strain gages embedded in the full-scale test slabs were compared with the computed strains from FE model developed. The strain at each gage location was computed using FE model by the application of static load shifted with the speed of HVS loading used for response measurements. A total of 64 shifts of pressure load 827.4 kPa (120 psi) were applied to simulate one pass of the HVS loading with a speed of 12 km/h (7.5 mph). Figure 7 shows the comparison between the analytical strains predicted using the FE model and the measured strains from the full-scale test slabs. Table 5 represents a summary of model parameters calibrated for the test slabs used in this study. The laboratory test results and calibrated parameters were used to perform the stress analysis under the critical loading condition in Florida circumstances.

6. Evalution of Potential Performance

Previous research on concrete pavements in Florida indicated that a typical severe temperature differential in the concrete slab at midday has been found to be about +11.1 °C (+20.0 °F). For this temperature condition, the most critical loading position is when the axle load is placed at the mid-edge of the slab (Tia et al. 1991). Conversely, concrete pavement slabs tend to have a negative temperature differential at night, and a typical severe temperature differential in the concrete slab at night has been found to be about −5.6 °C (−10.0 °F). For this temperature condition, the most critical loading position is when the axle load is placed at the corner of the slab.

Using these critical condition and the developed 3-D finite element models, critical stress analysis to determine the maximum stresses in each test slab under typical critical

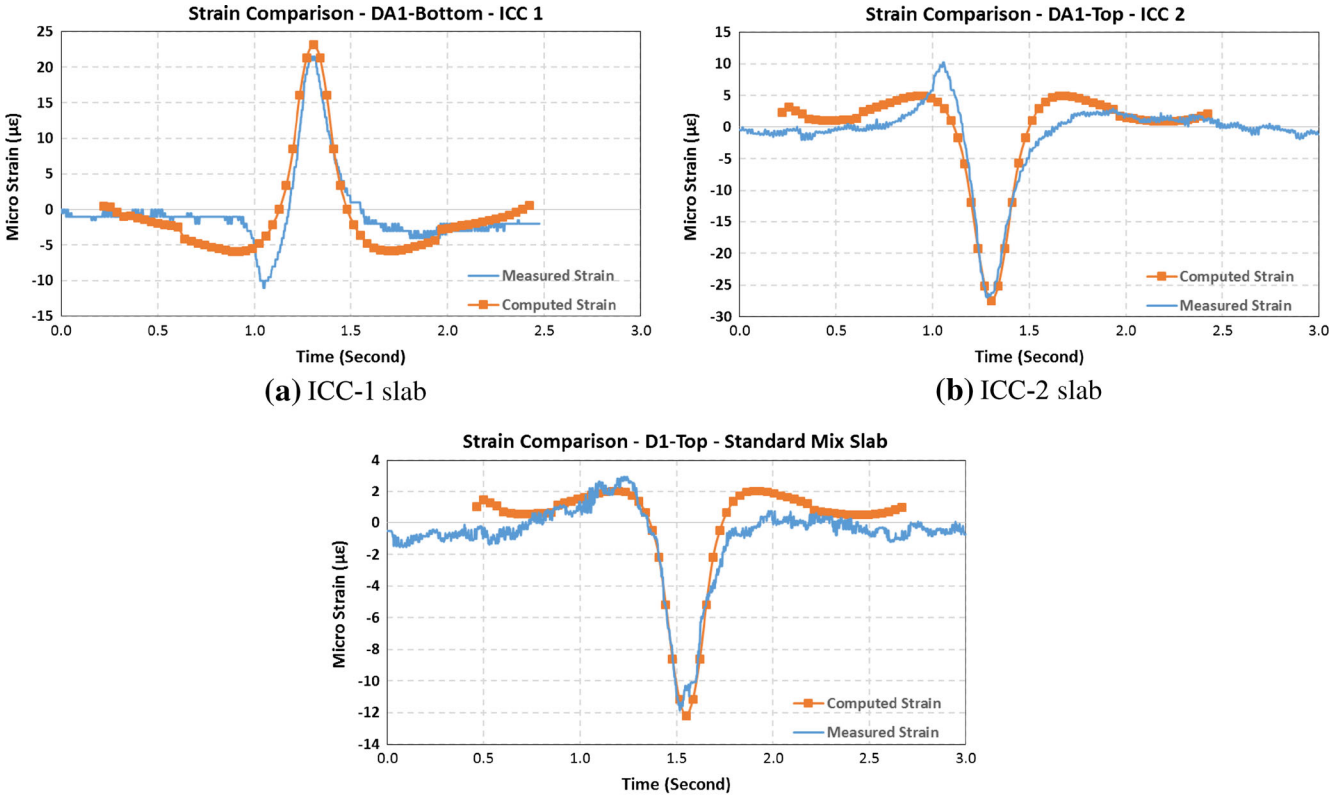

(a) ICC-1 slab

(b) ICC-2 slab

(c) Standard mix slab

Fig. 7 Measured and computed strains at selected gage locations.

temperature-load condition were performed with the calibrated parameters and the measured coefficient of thermal expansion of the each concrete mix used for each test slab. The flexural strength of the concrete determined in laboratory test was used to calculate the stress-to-strength ratio for analysis. A 98 kN (22-kip) single axle load which is the maximum legal axle load in Florida was used for analysis.

The potential performance of each test slab was evaluated based on the maximum stress-to-flexural strength ratio of the concrete. To calculate stress-to-strength ratio, the maximum computed stresses for the test slab were divided by the flexural strength of the respective concrete. According to the fatigue theory (Portland Cement Association 1984), the number of load repetitions to failure of concrete increases as the stress-to-strength ratio decreases. Thus, a lower computed stress-to strength ratio indicates better cracking performance. From the results presented in Table 6, it was identified that the computed stress-strength ratio of the ICC slabs were lower than that of the standard mix slab, which indicates a better potential performance of the ICC slab in the field.

7. Conclusions

In this study, a full-scale field experiment was conducted at the APT facility housed at the FDOT Material Research Park to evaluate the feasibility of using the ICC pavement in Florida. A total of three instrumented test slabs were constructed and tested using a HVS including two ICC slabs and one standard mix slab.

The structural response characteristics of the test slabs were evaluated using data obtained from the full-scale field tests. The temperature differentials of the ICC slabs are slightly higher than those of the standard mix slab likely due to the lower thermal conductivity of the ICC slabs. It appears that the addition of LWA as an internal curing agent increase the degree of hydration which results in a decrease in the thermal conductivity of the concrete. According to curling and environmental stain measurement results, the ICC concrete slabs generally show less curling movements and environmental strains.

In addition, the three-dimensional FE model was developed to analyze the mechanical behavior of the ICC and the standard mix concrete under Florida climate condition. The FE model developed was validated and calibrated using the HVS load-induced strains from the full-scale test sections. The verified model was then used to evaluate the potential performance of these test sections under critical temperature-load condition in Florida.

The maximum tensile stresses were computed using a 98 kN (22-kip) single axle load applied at the mid-edge of the slab with temperature differential of +11.1 °C (+20 °F) in the concrete slab. Based on the computed maximum stresses in the concrete, it is recommended that the ICC-1 mix design be the best to resist the critical load repetitions and therefore superior fatigue performance compared to the ICC-2 and the standard mix evaluated.

Table 6 Computed maximum stresses and stress-strength ratio.

Mix	Water-cement ratio	Coefficient of thermal expansion (m/m/°C)	Modulus of elasticity (MPa)	Modulus of rupture (kPa)	Computed stress (kPa)		Stress-to-strength ratio	
					Corner	Mid-edge	Corner	Mid-edge
Temperature differential of +11.1 °C (+20 °F) between top and bottom								
SM	0.40	7.965×10^{-6}	30,682	4999	1502	3110	0.30	0.62
ICC 1	0.32	7.630×10^{-6}	26,890	5654	1340	2740	0.24	0.48
ICC 2	0.40	7.630×10^{-6}	26,200	4861	1314	2687	0.27	0.55
Temperature differential of −5.6 °C (−10 °F) between top and bottom								
SM	0.40	7.965×10^{-6}	30,682	4999	1499	1067	0.30	0.21
ICC 1	0.32	7.630×10^{-6}	26,890	5654	1415	952	0.25	0.17
ICC 2	0.40	7.630×10^{-6}	26,200	4861	1407	936	0.29	0.19
Temperature differential of 0 °C (0 °F) between top and bottom								
SM	0.40	7.965×10^{-6}	30,682	4999	1195	1622	0.24	0.32
ICC 1	0.32	7.630×10^{-6}	26,890	5654	1137	1566	0.20	0.28
ICC 2	0.40	7.630×10^{-6}	26,200	4861	1126	1556	0.23	0.32

SM standard mix

Open Access

References

Bentz, D. P., Lura, P., & Roberts, J. W. (2005). Mixture proportioning for internal curing. *Concrete International, 27*(2), 35–40.

Bentz D. P., & Weiss, W. J. (2011). *Internal Curing: A State-of-the-Art Review*, National Institute of Standards and Technology [NIST].

Byard, B., & Schindler, A. K. (2010). *Cracking tendency of lightweight concrete,* Research report. University of Auburn, Auburn, AL.

Cusson, D., & Hoogeveen, T. (2008). Internal curing of high-performance concrete with pre-soaked fine lightweight aggregate for prevention of autogenous shrinkage cracking. *Cement Concrete Research, 38*(6), 757–765. doi:10.1016/j.cemconres.2008.02.001.

de Sensale, G. R., & Goncalves, A. F. (2014). Effects of Fine LWA and SAP as Internal Water Curing Agents. *International Journal of Concrete Structures and Materials, 8*(3), 229–238.

Lotfy, A., Hossain, K. M., & Lachemi, M. (2015). Lightweight self-consolidating concrete with expanded shale aggregates: Modelling and Optimization. *International Journal of Concrete Structures and Materials, 9*(2), 185–206.

Mehta, P. K., & Monteiro, P. J. (2013). *Concrete microstructure, properties, and materials* (4th ed.). New York, NY: McGraw-Hill Education.

Portland Cement Association, *Thickness Design for concrete Highway and Street Pavements*, Pulication No. EB109.01P, Slokie, IL, 1984.

Schlitter, J., Henkensiefken, R., Castro, J., Raoufi, K., Weiss, J., & Nantung, T. *Development of internally cured concrete for increased service life.* Publication FHWA/IN/JTRP-2010/10. Joint Transportation Research Program, Indiana Department of Transportation and Purdue University, West Lafayette, IN, 2010. doi:10.5703/1288284314262.

Tia, M., Bloomquist, D., Alungbe, GD., & Richardson, D. (1991). *Coefficient of thermal expansion of concrete used in Florida,* Research report. Gainesville, FL: University of Florida.

Tia, M., Wu, C. L., Ruth, B. E., Bloomquist, D., & Choubane, B. (1989). *Field evaluation of rigid pavements for the development of a rigid pavement design system-Phase IV,* Research report. Gainesville, FL: University of Florida.

Villarreal, V. H., & Crocker, D. A. (2007). Better pavements through internal hydration. *Concrete International, 29*(2), 32–36.

Weber, S., & Reinhardt, H. W. (1997). A new generation of high-performance concrete: Concrete with autogenous curing. *Advanced Cement Based Materials, 6*(2), 59–68. doi:10.1016/S1065-7355(97)00009-6.

Wei, Y., & Hansen, W. (2008). Pre-soaked lightweight fine aggregates as additives for internal curing in concrete. *American Concrete Institute, 256*, 35–44. https://www.concrete.org/publications/internationalconcreteabstractsportal.aspx?m=details&i=20229.

Weiss, W., Borischevsky, B., & Shah, S. (1999). *The influence of a shrinkage reducing admixture on the early-age behavior of high performance concrete," 5th International Symposium on the Utilization of High Strength/High performance Concrete*, (pp. 1418–1428) Sandefjord, Norway.